Isomerization and Decomposition Reactions of Primary Alkoxy Radicals Derived from Oxygenated Solvents

Melissa A. Ferenac, Andrew J. Davis, Andrew S. Holloway, and Theodore S. Dibble*

Department of Chemistry, State University of New York—Environmental Science and Forestry, 1 Forestry Drive, Syracuse, New York 13210

Received: June 12, 2002; In Final Form: October 7, 2002

This paper presents quantum chemical studies of the unimolecular isomerization (1,5 H-shift) and decomposition (β C−C scission) reactions of a series of six oxygenated alkoxy radicals and 1-butoxy radical. The goal is to better understand the effects of ether, carbonyl, and ester functional groups on the reactivity of alkoxy radicals relevant to atmospheric chemistry. We also report the first quantum chemical study of the α-ester rearrangement: $CH_3C(=O)OCH_2O^\bullet \rightarrow CH_3C(=O)OH + H\dot{C}=O$. The six radicals are $CH_3OC(=O)CH_2O^\bullet$, $CH_3C(=O)OCH_2O^\bullet$, $CH_3CH_2C(=O)CH_2O^\bullet$, $CH_3C(=O)CH_2CH_2O^\bullet$, $CH_3OCH_2CH_2O^\bullet$, and $CH_3CH_2OCH_2O^\bullet$. All these radicals are, like 1-butoxy, primary alkoxy radicals with a methyl group $\delta-$ to the radical center. Calculations are carried out at the B3LYP/6-31G(d,p) and /6-311G(2df,2p) level of theory for all reactions. In addition, the G2(MP2,SVP) level of theory is used to study all isomerization reactions and selected decomposition reactions. Substituent effects on structure are very large and certainly significant for the fate of these radicals in the atmosphere; fates depend as much or more on the position of functional groups as their identity. We also make a preliminary examination of the effects of tunneling on the computed rate constants for the α-ester rearrangement and the 1,5 H-shift reaction of 1-butoxy. At 298 K, we find tunneling to increase the rate of the 1,5 H-shift reaction by a factor of 19−210, and the rate of the α-ester rearrangement by a factor of 1.3 to 6. The effects of tunneling have been neglected in most previous computational studies of the 1,5 H-shift reaction.

I. Introduction

Oxygenated compounds, such as ethers and esters, are receiving increased attention for use as solvents and additives to diesel fuel and gasoline. Oxygenated organic compounds are present at high levels in the atmosphere;[1] some of these are directly emitted from anthropogenic sources, some are biogenic, and others are atmospheric degradation products of directly emitted compounds. While there have been a number of studies of the degradation of oxygenated solvents in environmental chambers,[2−10] the absence of authentic standards for many potential products limits the knowledge that can be gained from these studies. A better understanding of the effects of oxygen-substituents on the fate of radical intermediates formed in the degradation of oxygenated compounds would help fill the gaps in our understanding of their atmospheric chemistry. This knowledge will improve the reliability of chemical mechanisms used to model air pollution and develop ozone abatement strategies.

Degradation of volatile organic compounds (VOCs) in the atmosphere is typically initiated by reaction with an OH radical and, in the presence of NO_x, forms alkoxy radicals in high yield.[11] Alkoxy radicals constitute a critical branching point in the tropospheric oxidation of VOCs, because their fate is determined by the competition between reaction with O_2 and multiple unimolecular reactions. The most common reactions of alkoxy radicals are reaction with O_2, decomposition by β C−C bond fission, or isomerization via a 1,5 H-shift, as shown in Scheme 1.[11,12] The rate constants for the unimolecular isomerization and decomposition reactions are highly sensitive to molecular structure. The reaction pathways of alkoxy radicals may have a substantial effect on the extent of formation of ozone and secondary organic aerosol in polluted air.[13] Reaction with O_2 results in the prompt (seconds to minutes) formation of one molecule of ozone, but the unimolecular reactions propagate the organic radical chemistry, and have the potential to promptly produce two or more molecules of ozone. Alkoxy radical chemistry will also affect the formation of secondary organic aerosols, defined as those formed by gas-to-particle conversion. These aerosols are most likely to form from condensation of large compounds (those with low equilibrium vapor pressures)[14]

SCHEME 1

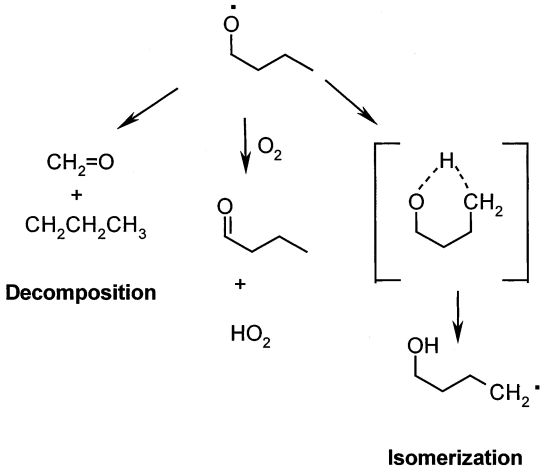

* Corresponding author. Fax: 315-470-6856. E-mail: tsdibble@syr.edu.

10.1021/jp0262923 CCC: $25.00
Published on Web 12/05/2002

and the decomposition reactions of alkoxy radicals tend to reduce the size of stable product compounds.

Although laser induced fluorescence (LIF) has been used to study the kinetics of alkoxy radical reactions for decades,[15] there are large gaps in the database of rate constants. Absolute rate constants for reactions of O_2 with small alkane-derived alkoxy radicals are well-known,[16−20] but only recently have absolute rate constants been determined for larger alkoxy radicals ($\geq C_4$).[21,22] Atkinson[12] and Zellner[23] suggest that 298 K rate constants for the O_2 reactions of alkane-derived alkoxy radicals are all approximately the same, with secondary alkoxy radicals being slightly more reactive than primary alkoxy radicals. Much, though not all, of the rate data on the unimolecular reactions of the larger alkoxy radicals consist of rates of reaction relative to the rate of the bimolecular reactions with O_2 or NO; the absolute rate constants for the unimolecular reaction can be obtained if one knows or estimates rate constants for the bimolecular reactions.[12] It has been established that isomerization reactions are relevant only for those molecules that can form a six-member, effectively strain-free, transition state.[12,24,25] Rates of decomposition reactions have been measured directly using laser-induced fluorescence to monitor the first-order rate of disappearance of alkoxy radicals produced by flash photolysis, but almost exclusively for the smaller members of the series of alkoxy radicals derived from alkanes.[26−29] Computations[30−32] and product yield studies[2−11,32] indicate that the activation barrier is significantly affected by the addition of functional groups.

In previous computational studies of alkoxy radical chemistry, we have relied upon density functional theory to provide efficient and reasonably reliable results, and we do so again here. Recently, Somnitz and Zellner[33−35] reported computational results for a number of aliphatic alkoxy radicals. They found that G2(MP2,SVP)[36] performed very well in calculating rate constants for alkoxy radical decomposition and isomerization reactions. We use this approach to check some of the B3LYP results.

This paper describes quantum mechanical investigations of the effects of oxygen-containing functional groups on the decomposition and isomerization of alkoxy radicals. We consider three pairs of *primary* alkoxy radicals, one pair derived from each of butanone, methyl ethyl ether, and methyl acetate. The reactions to be studied are show below.

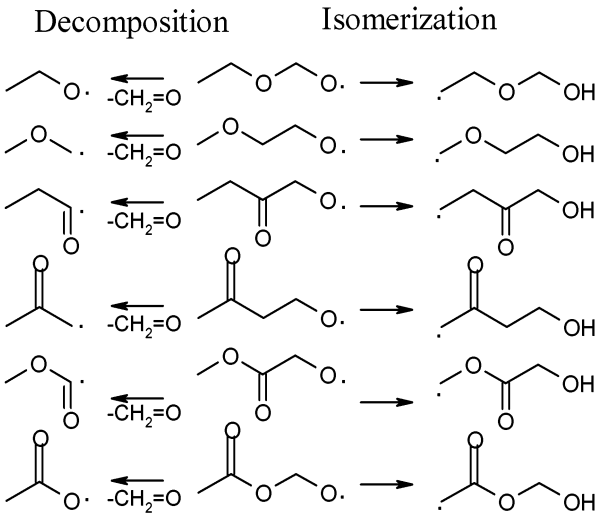

The results for these reactions are compared to the results for the decomposition and isomerization of 1-butoxy depicted in Scheme 1. In addition, we report the first quantum chemical study of the α-ester rearrangement, which has previously been observed in chamber experiments: [3,37−39]

$$CH_3C(=O)OCH_2O^{\bullet} \rightarrow CH_3C(=O)OH + H\dot{C}=O \quad (1)$$

Finally, we consider tunneling corrections to the rate constants for the isomerization reactions and the α-ester rearrangement.

II. Computational Methods

Molecular mechanics calculations were carried out using SPARTAN[40] to explore the conformational space of reactants and products, and the GAUSSIAN94[41] and GAUSSIAN98[42] series of programs were used for subsequent calculations. To find the most stable conformer of a radical, the 4−6 conformers reported as most stable by molecular mechanics were re-optimized using a 6-31G(d,p) basis set and density functional theory, specifically the correlation functional of Lee, Yang, and Parr[43] combined with the three-parameter hybrid exchange functional of Becke[44] (B3LYP). The unrestricted Hartree−Fock formalism was used for all radicals. The lowest energy conformer was used in subsequent B3LYP calculations.

First guesses for geometries of transition states for decomposition were obtained, starting from the B3LYP/6-31G(d,p) geometry of the corresponding radical, by increasing the length of the breaking C−C bond to ∼2.0 Å and performing a constrained optimization. The resulting geometry was then used for a direct and unconstrained transition state search. Transition states for isomerization were found by optimizing the geometry while constraining the length of both the breaking C−H bond and the forming O−H bond to ∼1.25 Å. The constraint was then released to carry out a direct transition state search.

Harmonic vibrational frequencies were calculated at B3LYP/6-31G(d,p) to verify the nature of potential energy minima and transition states, and were used without scaling to calculate zero-point energies (ZPE). Geometries were recalculated using the B3LYP/6-311G(2df,2p) approach. We recalculated activation barriers to all the isomerization reactions and three of the decomposition reactions using the G2(MP2,SVP)[45] approach. This method employs HF/6-31G(d) ZPEs and single-point calculations at MP2/6-31G(d) geometries (with all electrons correlated). The correlation energy is treated using QCISD(T)/6-31G(d) (frozen core) energies, and the effect of basis set on the QCISD(T) energy is estimated from an MP2/6-311+G(3df,2p) calculation. An empirical correction is used to further refine the energies (this term cancels out in the calculation of activation barriers). The conformational analysis of the reactant radicals was repeated at MP2/6-31G(d) for the G2(MP2,SVP) calculations.

Intrinsic reaction coordinate (IRC) calculations were used to verify the nature of the reaction for most, but not all, of the transition states studied. The transition states for the isomerization reactions possess very distinctive structures that are hard to confuse with other reactions, so we carried out few IRC calculations for those transition states. For each transition state where an IRC calculation was not carried out, the motion of the vibrational mode with an imaginary frequency was analyzed to confirm the nature of the transition state. IRC calculations were carried out for the α-ester rearrangement and all decomposition reactions.

The UNIMOL[46] program was used to calculate rate constants for the α-ester rearrangement of $CH_3C(=O)OCH_2O$. Lennard-Jones parameters were $\sigma = 5.4$ Å and $\epsilon = 549$ K, based on the recommendations of Gilbert and Smith[47] and the boiling points

TABLE 1: Absolute B3LYP Energies (Hartrees) at Two Basis Sets and Zero-Point Energies (ZPE, kcal/mol at 6-31G(d,p)) of Alkoxy Radicals, Transition States (TS), and Reaction Products for Isomerization (isom.) and Decomposition (decomp.)

species		6-31G(d,p)	ZPE	6-311G(2df,2p)
$CH_3CH_2CH_2CH_2O^\bullet$		−233.01132	77.0	−233.07974
isom.	TS	−232.99201	74.8	−233.06064
	product	−233.00813	77.2	−233.07877
decomp.	TS	−232.98378	75.0	−233.05524
	product	−118.48115	55.6	−118.51471
$CH_3OCH_2CH_2O^\bullet$		−268.89487	62.7	−268.97998
isom.	TS	−268.88256	60.4	−268.96751
	product	−268.90184	63.2	−268.99028
decomp.	TS	−268.87749	60.5	−268.96637
	product	−154.36896	41.4	−154.41998
$CH_3CH_2OCH_2O^\bullet$		−268.90862	62.1	−268.99434
isom.	TS	−268.87989	59.9	−268.96539
	product	−268.90258	61.9	−268.99163
decomp.	TS	−268.87455	60.8	−268.96077
	product	−154.37575	41.5	−154.42398
$CH_3C(=O)CH_2CH_2O^\bullet$		−307.02066	64.8	−307.11653
isom.	TS	−306.99613	62.7	−307.09201
	product	−307.02665	65.5	−307.12522
decomp.	TS	−306.99472	63.2	−307.09315
	product	−192.50223	44.2	−192.56244
$CH_3CH_2C(=O)CH_2O^\bullet$		−307.02156	65.1	−307.11804
isom.	TS	−306.99825	62.3	−307.09461
	product	−307.01317	64.3	−307.11289
decomp.	TS	−307.00950	63.6	−307.10907
	product	−192.50196	45.4	−192.56343
$CH_3OC(=O)CH_2O^\bullet$		−342.92898	50.7	−343.04167
isom.	TS	−342.90546	47.8	−343.01876
	product	−342.93209	50.2	−343.04824
decomp.	TS	−342.90256	49.0	−343.01855
	product	−228.40060	30.8	−228.47893
$CH_3C(=O)OCH_2O^\bullet$		−342.94635	50.3	−343.05968
isom.	TS	−342.90885	48.0	−343.02194
	product	−342.95421	51.7	−343.06932
decomp.	TS	−342.90764	48.1	−343.02187
	product	−228.41566	30.0	−228.49101
$CH_2=O$		−114.50320	16.8	−114.54320

of two similar alcohols ($CH_3C(=O)OCH_2CH_2OH$ and $CH_3OC(=O)CH_2OH$).

III. Results and Discussion

III. A. Relative Energies. B3LYP energies of the radicals, transition states, and products are given in Table 1. G2(MP2,SVP) energies of the radicals, transition states, and products are shown in Table 2. For simplicity, alkoxy radicals derived from ketones, ethers, and esters will be referred to in the text as ketone-oxy radicals, ether-oxy radicals, and ester-oxy radicals. Previous work has shown that calculations at the B3LYP/6-31G(d) or 6-31G(d,p) levels of theory produce fairly accurate activation barriers for many alkoxy radical *decomposition* (not necessarily isomerization) reactions,[30,48−51] while studies of decomposition using B3LYP with larger basis sets may tend to underestimate activation barriers but yield more accurate reaction energies.[33,49,51] It should be noted, however, that recent work raises questions about the accuracy of B3LYP for activation energies less than about 10 kcal/mol.[52,53] Little is known about basis set effects on relative energies for isomerization reactions at B3LYP, but results for 1-butoxy appear very good.[25,30,51] Therefore, activation barriers discussed in the text are those of the B3LYP/6-31G(d,p) basis set, and enthalpies of reaction are at B3LYP/6-311G(2df,2p), unless otherwise specified. The B3LYP results are not likely affected by spin contamination because the value of $\langle S^2 \rangle$ for B3LYP wave functions was always less than 0.76 for all radicals and transition states.

III. A. 1. Decomposition. Table 3 lists relative energies of decomposition in order of increasing B3LYP/6-31G(d,p) barrier height. As expected,[30,48−51] B3LYP activation barriers are always lower for the 6-311G(2df,2p) basis set than for the 6-31G(d,p) basis set; the differences are 0.3−2.4 kcal/mol.

Barrier heights for decomposition of all these radicals depend strongly on the position of the oxygen atoms relative to the breaking bond, as shown in Figures 1−3. For the ester-oxy and ketone-oxy radicals the barriers are lower by 7 and 8 kcal/mol, respectively, when the carbonyl carbon is bound to the leaving CH_2O group. An even greater effect is seen for the ether-oxy radicals, where the barrier is lower by 11 kcal/mol when oxygen is not bound to the leaving CH_2O group.

Figure 4 depicts the potential energy profile for the 1-butoxy radical. The B3LYP barrier height for 1-butoxy is 15.2 kcal/mol, about the same as that for $CH_3OC(=O)CH_2O^\bullet$ and $CH_3C(=O)CH_2CH_2O^\bullet$. $CH_3CH_2OCH_2O^\bullet$ and $CH_3C(=O)OCH_2O^\bullet$ are the only radicals with much higher barrier heights than 1-butoxy.

As can be seen from Figures 1−4 and Table 3, all B3LYP values of the enthalpy of decomposition at 0 K ($\Delta_r H$ (0 K)), are positive. Results at 6-311G(2df,2p) are 1.2−3.7 kcal/mol lower than those at 6-31G(d,p). The reaction enthalpies are less dependent upon the functional group present and its position than are the activation barriers. Values of $\Delta_r H$ (0 K) for ketone-oxy radicals are lower than those for the ether-oxy and ester-oxy radicals. For ketone-oxy radicals and ether-oxy radicals that yield products with their radical centers on methylene groups, $\Delta_r H$ (0 K) is lower than the corresponding reaction which

TABLE 2: Absolute G2(MP2,SVP) Energies (Hartrees) of Alkoxy Radicals and Transition States for Isomerization Reactions, and Transition States and Products for Selected Decomposition (decomp.) Reactions

	G2(UMP2,SVP)		G2(PMP2,SVP)	
radical	reactant	TS	reactant	TS
$CH_3CH_2CH_2CH_2O^\bullet$	−232.62714	−232.61490	−232.62755	−232.61544
$CH_3OCH_2CH_2O^\bullet$	−268.52196	−268.51772	−268.52236	−268.51829
decomp.		−268.51602		−268.51570
$CH_3CH_2OCH_2O^\bullet$	−268.54310	−268.51779	−268.54360	−268.51831
$CH_3CH_2C(=O)CH_2O^\bullet$	−306.60367	−306.58660	−306.60415	−306.58713
decomp.		−306.60077		−306.60085
$CH_3C(=O)CH_2CH_2O^\bullet$	−306.60854	−306.58539	−306.60904	−306.58566
$CH_3OC(=O)CH_2O^\bullet$	−342.52741	−342.50656	−342.52788	−342.50711
$CH_3C(=O)OCH_2O^\bullet$	−342.54685	−342.50773	−342.54735	−342.50817

reaction products	G2(UMP2,SVP)	G2(PMP2,SVP)
$CH_3CH_2C(=O)^\bullet$	−192.23005	−192.23019
$CH_3OCH_2^\bullet$	−154.13630	−154.13638
$CH_2=O$	−114.37248	−114.37248

TABLE 3: Barrier Heights ($E^{\neq}$) and Enthalpies of Reaction ($\Delta_r H$) at 0 K in kcal/mol for Decomposition Reactions of Alkoxy Radicals Using B3LYP and G2(MP2,SVP)

	$E^{\neq}$				$\Delta_r H$ (0 K)			
	B3LYP		G2(MP2,SVP)		B3LYP		G2(MP2,SVP)	
radical	6-31G(d,p)	6-311G (2df,2p)	UMP2	PMP2	6-31G(d,p)	6-311G (2df,2p)	UMP2	PMP2
$CH_3CH_2C(=O)CH_2O^{\bullet}$	6.1	4.1	1.8	2.1	7.3	4.2	0.7	0.9
$CH_3OCH_2CH_2O^{\bullet}$	8.7	6.3	3.7	4.2	9.8	6.1	8.3	8.5
$CH_3C(=O)CH_2CH_2O^{\bullet}$	14.6	13.0			5.7	3.0		
$CH_3OC(=O)CH_2O^{\bullet}$	14.9	12.8			12.6	9.1		
$CH_3CH_2CH_2CH_2O^{\bullet}$	15.2	13.3		15.0[a]	12.3	9.0		
$CH_3CH_2OCH_2O^{\bullet}$	20.1	19.8			14.8	13.2		
$CH_3C(=O)OCH_2O^{\bullet}$	22.1	21.5	36.6	26.7	13.7	12.4		

[a] Reference 34.

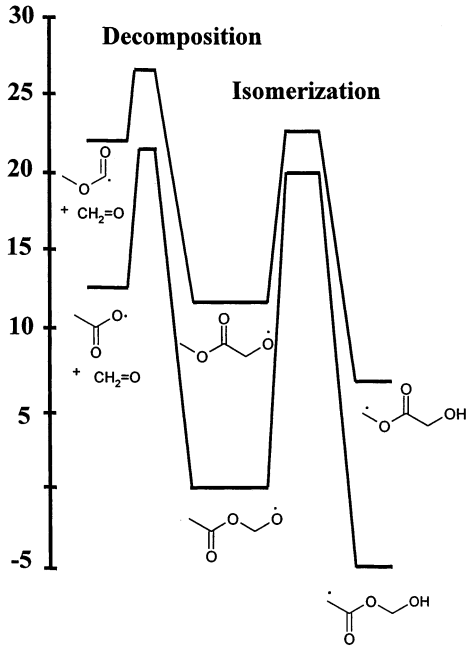

Figure 1. Potential energy profiles (kcal/mol) for the decomposition and isomerization reactions of $CH_3C(=O)OCH_2O^{\bullet}$ and $CH_3OC(=O)CH_2O^{\bullet}$ at B3LYP. The relative energies of $CH_3C(=O)OCH_2O^{\bullet}$ and $CH_3OC(=O)CH_2O^{\bullet}$ are as indicated in the figure.

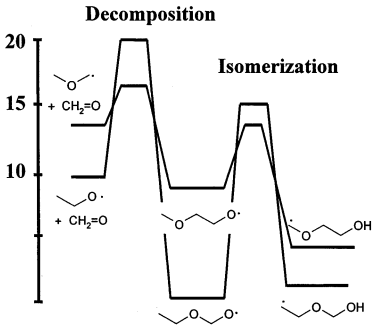

Figure 2. Potential energy profiles (kcal/mol) for the decomposition and isomerization reactions of $CH_3CH_2OCH_2O^{\bullet}$ and $CH_3OCH_2CH_2O^{\bullet}$ at B3LYP. The relative energies of $CH_3CH_2OCH_2O^{\bullet}$ and $CH_3OCH_2CH_2O^{\bullet}$ are as indicated in the figure.

produces radicals centered on carbonyl groups or oxygen atoms. Therefore, the radical with the lowest barrier to decomposition ($CH_3CH_2C(=O)CH_2O^{\bullet}$) is not the radical with the most negative enthalpy of reaction. Although one might assume that resonance stabilization in the $CH_3C(=O)O^{\bullet}$ radical makes it more stable than the $CH_3O\dot{C}(=O)$ radical, the heats of reaction obtained here contradict that expectation.

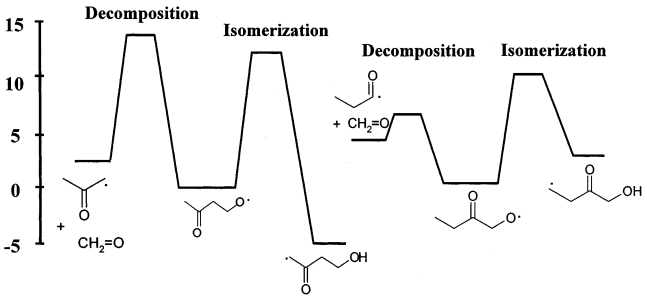

Figure 3. Potential energy profiles (kcal/mol) for the decomposition and isomerization reactions of $CH_3C(=O)CH_2CH_2O^{\bullet}$ and $CH_3CH_2C(=O)\ CH_2O^{\bullet}$ at B3LYP. The relative energies of $CH_3C(=O)CH_2CH_2O^{\bullet}$ and $CH_3CH_2C(=O)\ CH_2O^{\bullet}$ are as indicated in the figure.

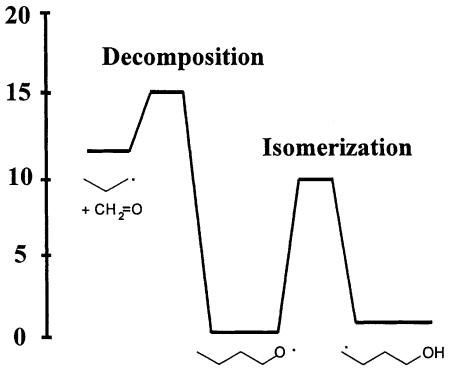

Figure 4. Potential energy profiles (kcal/mol) for the decomposition and isomerization reactions of 1-butoxy radical ($CH_3CH_2CH_2CH_2O^{\bullet}$) at B3LYP.

The barrier heights for the ether-oxy and ester-oxy radicals follow Hammond's postulate. In fact, considering all seven radicals, the only significant deviation from Hammond's postulate[54] is for $CH_3C(=O)CH_2CH_2O^{\bullet}$, which has a much larger barrier height than would be expected from its enthalpy of decomposition.

Activation barriers of decomposition were calculated using the G2(MP2,SVP) method only for $CH_3CH_2C(=O)CH_2O^{\bullet}$, $CH_3OCH_2CH_2O^{\bullet}$, and $CH_3C(=O)OCH_2O^{\bullet}$. Wave functions for the transition states were severely contaminated by higher-lying spin states, with values of $\langle S^2 \rangle$ of 0.97, 0.88, and 0.93, respectively. Looking only at the first two of these three compounds, it can be seen from Table 3 that using PMP2 rather than UMP2 energies creates only very small differences in the G2(MP2,SVP) energies, and B3LYP activation energies are ~4 kcal/mol higher than G2(MP2,SVP). In the case of $CH_3C(=O)OCH_2O^{\bullet}$, projecting the spins lowers the activation energy by fully 10 kcal/mol, still leaving it 5 kcal/mol higher in energy than the B3LYP/6-31G(d,p) value.

TABLE 4: Barrier Heights ($E^{\neq}$) and Enthalpies of Reactions ($\Delta_r H$) at 0 K in kcal/mol for Isomerization Reactions of Alkoxy Radicals Using B3LYP and G2(MP2,SVP)

	$E^{\neq}$				$\Delta_r H$ (0 K)	
	B3LYP		G2(MP2,SVP)		B3LYP	
radical	6-31G(d,p)	6-311G (2df,2p)	UMP2	PMP2	6-31G(d,p)	6-311G (2df,2p)
$CH_3OCH_2CH_2O^{\bullet}$	5.5	5.6	2.7	2.6	−3.9	−6.0
$CH_3CH_2CH_2CH_2O^{\bullet}$	9.9	9.8	7.7	7.6	2.2	0.4
$CH_3CH_2C(=O)CH_2O^{\bullet}$	11.8	11.9	10.7	10.7	4.5	2.5
$CH_3OC(=O)CH_2O^{\bullet}$	11.8	11.4	13.1	13.0	−2.4	−4.6
$CH_3C(=O)CH_2CH_2O^{\bullet}$	13.2	13.2	14.5	14.7	−3.1	−4.8
$CH_3CH_2OCH_2O^{\bullet}$	15.8	16.0	15.9	15.9	3.5	1.4
$CH_3C(=O)OCH_2O^{\bullet}$	21.2	21.3	24.6	24.6	−3.5	−4.7

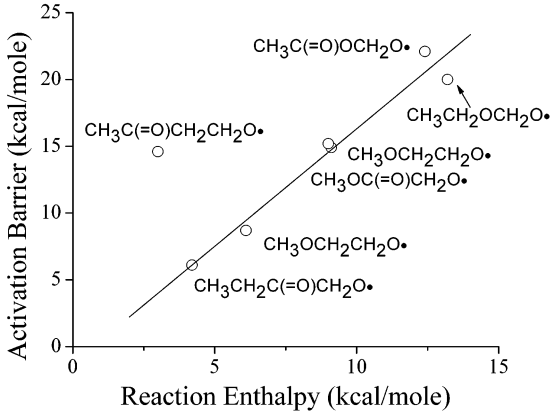

Figure 5. Relationship between B3LYP activation barrier to decomposition (6-31G(d,p) and reaction enthalpy 6-311G(2df,2p) at 0 K). The trend line is based on all the alkoxy radicals except $CH_3C(=O)CH_2CH_2O^{\bullet}$.

Atkinson[12] proposed a structure−activity relationship (SAR) for the activation barrier, E_0, to decomposition of alkoxy radicals:

$$E_0\ (\text{kcal/mol}) = a + b\Delta_r H \qquad (2)$$

with recommendations for a and b of

$$a = 2.4(\text{IP}) - 8.1, \text{ and } b = 0.36 \qquad (3)$$

where IP is the ionization potential (in eV) of the radical produced in the decomposition and $\Delta_r H$ is the standard enthalpy change for the reaction in kcal/mol (at 298 K). Typical values of a are 11.3 kcal/mol for primary alkyl radicals and 9.3 kcal/mol for secondary alkyl radicals. The IPs of the radical products of the decomposition reactions studied here are expected to vary considerably, because they possess very different substituents and the radical center is sometimes associated with a carbon atom and sometimes with an oxygen atom. Therefore, we should not expect a simple plot of activation barrier versus reaction energy to show a good correlation. However, as shown in Figure 5, six of the seven points lie very close to a single trend line, defined by

$$E_0 = -1.29\ \text{kcal/mol} + 1.76\ \Delta_r H \qquad (4)$$

where we used $\Delta_r H$ at 0 K instead of 298 K.

The rms deviation for these six radicals is 5.8% and the maximum error is 8.9%. The single alkoxy radical for which this relationship works very poorly is $CH_3C(=O)CH_2CH_2O^{\bullet}$. (Recall that this radical is the only one of the seven alkoxy radicals to significantly violate Hammond's postulate.)[54] However, Hammond's postulate does not take into account interactions of the electronic configurations of the reactant and product, differences which are significant in this case.[55,56] It may also be the case that the stability imparted to the $CH_3C(=O)CH_2^{\bullet}$ product of the decomposition reaction by the presence of two resonance structures is not realized in the transition state; this issue has been discussed by Vereecken and Peeters in the context of H-atom abstraction from allylic sites in alkenes.[57] The differences between Atkinson's recommendations and these values of a and b are quite large, and may reflect, in part, some bias in the B3LYP treatment of these reactions (we assume that the effect of temperature on $\Delta_r H$ is not significant here). To the extent that these results are valid, they seem to contradict the notion of including a term for ionization potential in the SAR. It should be noted that the activation barriers used were the B3LYP/6-31G(d,p) values and the reaction enthalpies used were B3LYP/6-311G(2df,2p) values, both at 0 K. The use of two different basis sets is in accord with the arguments given in the Computational Methods section as to which was expected to give the more accurate values. However, a comparison of the results in Table 3 with the results of higher level calculations[33] and the thermodynamic data used by Atkinson[12] implies that in the case of 1-butoxy, 6-31G(d,p) appears to give a more accurate reaction enthalpy than 6-311G(2df,2p). Nevertheless, recent modifications to Atkinson's SAR by Aschmann and Atkinson offer some reason to believe that the strong correlation seen in Figure 5, and the very different value of a obtained here, are not solely artifacts of the B3LYP method. They considered alkoxy radicals of the type $ROC(O^{\bullet})R'R''$ undergoing decomposition reactions in which the radical leaving group was an alkoxy radical (as in $CH_3CH_2OCH_2O^{\bullet}$). To account for experimental product yields they found it necessary to lower the value of a (the IP-dependent term) in Atkinson's SAR to a value intermediate between the recommendation for primary alkyl radicals and that for secondary alkyl radicals. In fact, alkoxy radicals have IPs significantly higher than alkyl radicals.[58−60]

III. A. 2. Isomerization. Relative energies of isomerization are shown in Table 4, and listed in order of increasing B3LYP/6-31G(d,p) activation energy. Figures 1−4 depict the potential energy profiles for isomerization alongside those for decomposition. B3LYP activation energies differ remarkably little between basis sets. Results are again more dependent upon the placement of the functional group than on the nature of that group, except for the ketone-oxy radicals, for which the placement of the carbonyl group makes little difference. The activation barrier for the ether-oxy and ester-oxy radicals are lower by ∼10 kcal/mol when the oxygen is adjacent to the methyl group from which abstraction occurs than when it is closer to the alkoxy radical center. It is interesting that the same structural element lowers the barrier to decomposition of these radicals to roughly the same degree.

TABLE 5: Absolute Energies (Hartrees) and Zero-Point Energies (ZPE, kcal/mol), of Alkoxy Radical, Transition State (TS), and Products for the α-Ester Rearrangement

	B3LYP			G2(MP2,SVP)	
species	6-31G(d,p)	ZPE	6-311G (2df,2p)	UMP2	PMP2
$CH_3C(=O)OCH_2O^\bullet$	−342.94635	50.3	−343.05968	−342.54685	−342.54734
TS	−342.92917	47.6	−343.04385	−342.52903	−342.52977
$HC^\bullet O$	−113.85183	8.2	−113.89304		
$CH_3C(=O)OH$	−229.09147	38.9	−229.17004		

TABLE 6: Barrier Heights ($E^{\neq}$) and Enthalpies of Reactions ($\Delta_r H$) at 0 K in kcal/mol for the α-Ester Rearrangement Using B3LYP and G2(MP2,SVP)

$E^{\neq}$				$\Delta_r H$ (0 K)			
B3LYP		G2(MP2,SVP)		B3LYP		G2(MP2,SVP)	
6-31G(d,p)	6-311G (2df,2p)	UMP2	PMP2	6-31G(d,p)	6-311G (2df,2p)	UMP2	PMP2
8.0	7.2	11.2	11.0	−1.4	−5.4	−7.6	−7.4

1-Butoxy has a B3LYP activation energy to isomerization of 9.9 kcal/mol at 6-31G(d,p), and only $CH_3OCH_2CH_2O^\bullet$ has a lower barrier. Recall that, for decomposition, 1-butoxy has the third highest activation barrier and $CH_3CH_2OCH_2O^\bullet$ the second highest. $CH_3OC(=O)CH_2O^\bullet$ has the same activation energy (11.8 kcal/mol) as the isoelectronic ketone-oxy radical with the carbonyl group in the same position ($CH_3CH_2C(=O)CH_2O^\bullet$).

Enthalpies of isomerization at 6-311G(2df,2p) are commonly 2 kcal/mol more negative than 6-31G(d,p) values, which represents a much bigger basis set effect than the differences in activation energies. Structure effects on energies of reaction for ketone-oxy radicals are surprising when compared to activation energy; the pair of ketone-oxy radicals violate Hammond's postulate (as they do for decomposition reactions): the ketone with the lower activation energy undergoes an endoergic reaction, and the one with the highest activation energy undergoes an exoergic reaction. The ether-oxy radicals follow Hammond's rule, but the activation barriers for the ester-oxy radicals differ by ∼9 kcal/mol despite having the same $\Delta_r H$ (0 K).

We examined our data to determine whether there existed a relationship between reaction energy and activation barrier to isomerization similar to that described previously for the decomposition reaction. The narrow distributions of reaction energies do not sustain any convincing correlation. We do see correlations, similar to those developed for substituent effects on rates of H-atom abstraction by OH, between pairs of alkoxy radicals with the same functionality: an ether linkage activates an adjacent $-CH_3$ group and the presence of a carbonyl group deactivates an adjacent $-CH_3$ group.[61]

Activation barriers to isomerization, but not reaction enthalpies, were calculated using the G2(MP2,SVP) method for all molecules studied. Table 4 includes results calculated using both the UMP2 and PMP2 energies, the small effect of spin projection is consistent with the modest extent of spin contamination in the transition states ($\langle S^{**}2\rangle = 0.78-0.80$). Differences between B3LYP and G2(MP2,SVP) activation barriers for isomerization are never more than 2.4 kcal/mol. G2(MP2,SVP) yields lower barriers than B3LYP for the reactions with low barriers (<10−13 kcal/mol).

III. A. 3. α-Ester Rearrangement. Absolute energies of the $CH_3C(=O)OCH_2O^\bullet$ α-ester rearrangement are shown in Table 5 and relative energies are listed in Table 6. The G2(MP2,-SVP) barrier height of 11.0 kcal/mol is significantly higher than the B3LYP values of 8.0 and 7.2 using the 6-31G(d,p) and 6-311G(2df,2p) basis sets, respectively. There is little spin contamination in either the B3LYP or Hartree−Fock wave functions, so there is only a small (0.2 kcal/mol) difference between the G2(UMP2,SVP) and G2(PMP2,SVP) barrier heights.

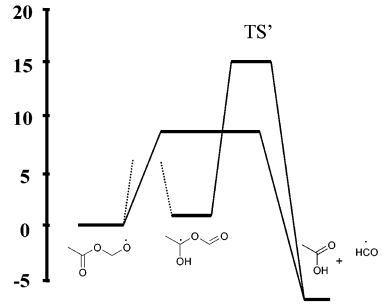

Figure 6. Potential energy profile for the two possible mechanisms of the its α-ester rearrangement of $CH_3C(=O)OCH_2O^\bullet$. The dashed lines connect $CH_3C(=O)OCH_2O^\bullet$ to the first transition state in the two-step mechanism proposed for the reaction; as the structure of this transition state was never obtained, it is not shown in this figure.

The transition state for the $CH_3C(=O)OCH_2O^\bullet$ α-ester rearrangement is that of a concerted mechanism; we also considered a two-step reaction sequence:

$$CH_3C(=O)OCH_2O^\bullet \rightarrow [TS] \rightarrow CH_3\dot{C}(OH)OCH(=O) \quad (5)$$

$$CH_3\dot{C}(OH)OCH(=O) \rightarrow [TS]' \rightarrow CH_3C(=O)OH + H\dot{C}(=O) \quad (6)$$

The B3LYP/6-31G(d,p) energy of the radical product of reaction 5, above, is only 1.0 kcal/mol higher than the energy of $CH_3C(=O)OCH_2O^\bullet$. However, as shown in Figure 6, the activation energy of the decomposition of this intermediate via TS′ is 7.6 kcal/mol higher than the activation energy of the concerted mechanism. Therefore, we can conclude that the α-ester rearrangement proceeds via the concerted mechanism for $CH_3C(=O)OCH_2O^\bullet$. Spin contamination was small, with $\langle S^2\rangle$ less than 0.76 and 0.78 for B3LYP and Hartree−Fock, respectively.

Experimental evidence for the occurrence of the α-ester rearrangement and near-absence of the β-ester rearrangement[2,3,37,38] might seem odd in light of the much more favorable six-member ring of the latter reaction; strain energy in the five-member transition state is the primary reason the 1,4 H-shift reaction is insignificant in comparison to the 1,5 H-shift.[11,12,25,51] Some insight may be gained from the depiction of the B3LYP/6-31G(d,p) potential energy profile along the reaction coordinate in Figure 7. As the reactant evolves toward the transition state

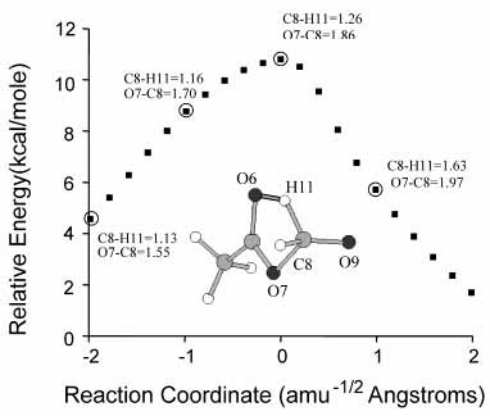

Figure 7. Electronic energy along the reaction coordinate for the α-ester rearrangement of $CH_3C(=O)OCH_2O^•$. Bond lengths for the breaking C−O and C−H bonds are given at selected points (indicated by the circles).

the extension of the breaking C−H bond is small relative to the extension of the breaking O7−C8 bond. Consideration of the structural changes upon lengthening the $CH_3C(=O)O-CH_2O^•$ bond suggests the following: lengthening this bond creates radical character of the carbonyl oxygen of the radical (O6 in Figure 7), which causes the oxygen to become reactive: the Mulliken spin densities in the transition state at O6 is 0.22, while that of the original radical center (O9) is 0.47. The spin density of O7, which would be the radical center in the decomposition product, is only 0.03. The absence of a β-ester rearrangement in $RC(=O)OCH_2CHR'O^•$ compounds is then rationalized in terms of the absence of any radical character on the carbonyl oxygen.

In fact, minimizing the radical energy at increasingly stretched $CH_3C(=O)O-CH_2O^•$ bond lengths leads to the α-ester rearrangement whenever a hydrogen atom is suitably positioned to transfer. The transition state for the decomposition reaction:

$$CH_3C(=O)OCH_2O^• \rightarrow CH_3C(=O)O^• + CH_2O \qquad (7)$$

which is significantly higher in energy than the transition state for the concerted α-ester rearrangement, can only be reached from conformations that orient both hydrogen atoms of the CH_2O group away from the carbonyl group, as shown in Figure 8.

III. B. Trends in Transition State Geometries and Relationship to Reactivity. B3LYP geometries may be found in the Supporting Information. The structures of the transition states are discussed below.

III. B. 1. Decomposition. The structure of the transition state for decomposition of $CH_3CH_2OCH_2O^•$ is shown in Figure 9, and that for $CH_3C(=O)OCH_2O^•$ in Figure 8. The lengths of the breaking bonds for transition states are shown in Table 7, in order of increasing B3LYP/6-31G(d,p) activation energy. The B3LYP values of the breaking bond length in the TS are very consistent between basis sets except for where the 6-31G(d,p) basis set suggests lengths greater than 2.2 Å; here, the larger basis set yields much smaller distances. For two transition states showing such long breaking C−C distances in the transition state, the MP2 calculation suggests those C−C distances are 0.2−0.3 Å shorter than the B3LYP/6-31G(d,p) values. For $CH_3C(=O)OCH_2O^•$, the MP2 value of the breaking C−O bond distance is only 0.02 Å shorter than the B3LYP value of 1.83 Å. Both B3LYP and MP2 show the same ordering in the lengths of the breaking bonds. There is no correlation between functional group and bond length, and little correlation between activation energies and bond lengths.

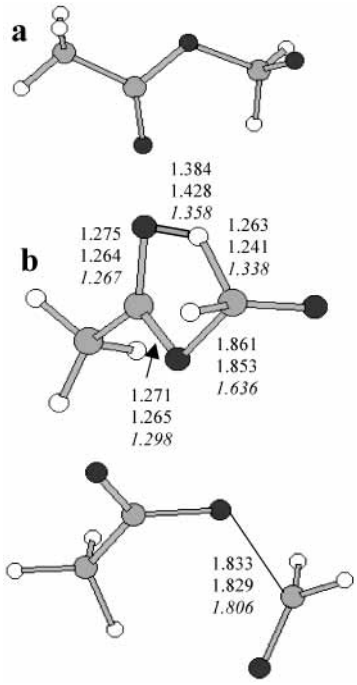

Figure 8. Structures of species on the potential energy surface of the $CH_3C(=O)OCH_2O^•$ radical: (a) the structure of the most stable conformer of the radical, (b) the transition state for its α-ester rearrangement, (c) the transition state for its decomposition reaction. Critical bond lengths of the transition states are reported for B3LYP/6-31G(d,p) and B3LYP/6-311G(2df,2p), in that order. MP2(full)/6-31G-(d) values are reported in italics.

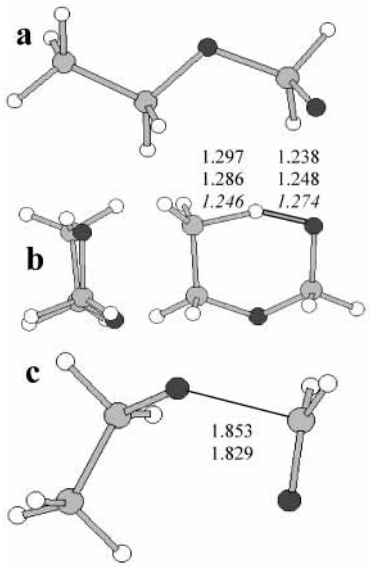

Figure 9. Structures of species on the potential energy surface of the $CH_3CH_2OCH_2O^•$ radical: (a) the structure of the most stable conformer of the radical, (b) two views of the transition state for its isomerization reaction, (c) the transition state for its decomposition reaction. Critical bond lengths of the transition states are reported for B3LYP/6-31G-(d,p) and B3LYP/6-311G(2df,2p), in that order. MP2(full)/6-31G(d) values, where available, are reported in italics.

III. B. 2. Isomerization. Two views of the structure of the six-member transition state for isomerization of $CH_3CH_2-OCH_2O^•$ are shown in Figure 9b. As is typical of the transition states not constrained by a C=O double bond, four of the six atoms of the transition state lie nearly in a plane, with the

TABLE 7: Length of the Breaking Bond (Å) in the Transition State for Decomposition of Alkoxy Radicals, in Order of Increasing B3LYP/6-31G(d,p) Barrier Height

reactant	B3LYP/ 6-31G(d,p)	B3LYP/ 6-311G(2df,2p)	MP2(full)/ 6-31G(d)
$CH_3CH_2C(=O)CH_2O^\bullet$	2.26	2.19	1.95
$CH_3OCH_2CH_2O^\bullet$	2.32	2.22	2.05
$CH_3C(=O)CH_2CH_2O^\bullet$	2.09	2.07	
$CH_3OC(=O)CH_2O^\bullet$	2.21	2.17	
$CH_3C(=O)OCH_2O^\bullet$	1.83	1.83	1.81
$CH_3CH_2CH_2CH_2O^\bullet$	2.23	2.18	
$CH_3CH_2OCH_2O^\bullet$	1.85	1.83	

shifting H-atom only slightly out of the plane. Critical bond lengths in the transition state are shown in Tables 8 and 9 at all levels of theory employed. There are only slight variations in lengths of breaking/forming bonds between molecules at a given level of theory, and no trend with activation energy or energy of reaction. The MP2 transition states are slightly more like reactants than the B3LYP transition states.

III. B. 3. α*-Ester Rearrangement.* Figure 8 illustrates the structure of the transition state for the α-ester rearrangement and for decomposition, and lists the length of critical bonds in the transition states at various levels of theory. The MP2 structure of the transition state is significantly different from the B3LYP structure: the breaking O−C bond is ∼0.2 Å shorter at MP2 and the transferred H-atom is ∼0.1 Å further from the carbon atom. While some of the difference in the C−H distance might be due to the absence of *p* polarization functions in the MP2 geometry calculation, that would not explain the large difference in the O−C distance. The length of the breaking O−C bond (at B3LYP) is nearly the same for the α-ester rearrangement as it is for decomposition.

III. C. Atmospheric Fate of Alkoxy Radicals. It is known from previous calculations that the Arrhenius *A* factors for isomerization and decomposition are in the range $10^{11.9-12.3}$ s^{-1} and $10^{13.0-13.3}$ s^{-1}, respectively (at 1 atm and 298 K).[30−35,51] Activation barriers derived from quantum computations are usually very close to, and generally within 1 kcal/mol of, the values obtained upon carrying out an RRKM calculation of the rate constant at 1 atm.[34,35,51] This may not hold for the lowest activation energies (fastest reactions), but in these cases the error will not alter the conclusions of our kinetic analysis unless the barriers to both isomerization and decomposition are very low. Therefore, the atmospherically relevant rate constants for these reactions can be estimated using the *A* factors cited above and the activation barriers listed in Tables 3 and 4.

For 1-butoxy, the calculations presented here (and those of other groups)[30,34,35] suggest rate constants for isomerization (∼10^5 s^{-1}) and decomposition (∼10^1 s^{-1}) that agree with the experimental finding that there is no decomposition and that isomerization outcompetes the O_2 reaction by a factor of ∼3.[62−64] The O_2 reaction of most alkoxy radicals is supposed to occur with a rate constant of about $6-10 \times 10^{-15}$, corresponding to a pseudo-first-order rate constant of 2×10^4 s^{-1} in 1 atm of air.[23] However, this conclusion is based on measurements for alkane-derived alkoxy radicals only, and results from our laboratory suggest that the rate constant should not be assumed constant even for members of this class of radicals.[21,22] Aschmann and Atkinson suggested, on the basis of thermodynamic arguments, that k_{O_2} is 2−3 times higher for alkoxy radicals of the type R−CH(O•)OR.[2] In the absence of experimental data we will assume that the rate constant does not differ from the recommended value in these radicals by more than an order of magnitude.

The potential energy profiles for the isomerization and decomposition reactions of the alkoxy radicals were shown in Figures 1−4. By inspection of these figures and Table 4, and by comparison to 1-butoxy, it is clear that of all the oxygenated alkoxy radicals studied herein, only for $CH_3OCH_2CH_2O^\bullet$ does isomerization outcompete O_2 reaction ($k_{iso} \sim 10^8$ s^{-1} at B3LYP and 10^{10} at G2(MP2,SVP)). However, the computed barrier for decomposition is only 2−3 kcal/mol higher than that for isomerization. Given that the *A*-factor for decomposition is about 10 times higher than that for isomerization, the isomerization reaction is computed to be favored by a factor of only 3−10 at 298 K. Also, considering the uncertainties in the calculated activation barriers, it is quite possible that decomposition constitutes a significant reaction pathway of this radical, nor would it be entirely surprising if decomposition was found to be faster than isomerization.

For two other compounds, $CH_3CH_2C(=O)CH_2O^\bullet$ and $CH_3OC(=O)CH_2O^\bullet$, activation barriers to isomerization are computed to be about 12 kcal/mol at B3LYP, and 9 and 13 kcal/mol, respectively, at G2(MP2,SVP). The B3LYP barrier heights, if taken at face value, would imply that isomerization is somewhat slower than the expected rate of the O_2 reaction, while the G2(MP2,SVP) result for $CH_3CH_2C(=O)CH_2O^\bullet$ implies isomerization to be faster than the O_2 reaction. However, for $CH_3CH_2C(=O)CH_2O^\bullet$, the computed activation barrier to decomposition of 4 kcal/mol implies a rate constant of 10^{10} s^{-1}, 5 orders of magnitude faster than the expected rate of the O_2 reaction. None of the other alkoxy radicals studied here has a barrier to decomposition sufficiently low to make decomposition faster than the O_2 reaction. Isomerization might be nonnegligible for $CH_3OC(=O)CH_2O^\bullet$, if the computed barriers are too high or if the O_2 reaction is slower than it appears to be for alkane-derived alkoxy radicals.

The computed barrier for the α-ester rearrangement of $CH_3C(=O)OCH_2O^\bullet$ ranges from 7.2 to 11.2 kcal/mol, depending on the level of theory, and there are no previous estimates of the *A* factor. The results of our RRKM-Master Equation calculations are presented in Figure 10 for a range of assumed activation barriers. Figure 10 also displays results inferred from recent chamber studies.[37,39] If the O_2 reaction is occurring at the rate commonly assumed (that of ethoxy radical), it implies an activation barrier of ∼10.5 kcal/mol. If the rate constant is a

TABLE 8: Critical Bond Lengths in the Transition State for Isomerization of Alkoxy Radicals at B3LYP, in Order of Increasing B3LYP/6-31G(d,p) Barrier Height

	B3LYP/6-31G(d,p)			B3LYP/6-311G(2df,2p)		
radical	*r*(C−H)	*r*(O−H)	*r*(O−C)	*r*(C−H)	*r*(O−H)	*r*(O−C)
$CH_3OCH_2CH_2O^\bullet$	1.295	1.261	2.456	1.284	1.272	2.457
$CH_3CH_2CH_2CH_2O^\bullet$	1.304	1.226	2.460	1.291	1.237	2.461
$CH_3CH_2C(=O)CH_2O^\bullet$	1.314	1.207	2.453	1.302	1.217	2.454
$CH_3OC(=O)CH_2O^\bullet$	1.302	1.203	2.421	1.288	1.210	2.423
$CH_3C(=O)CH_2CH_2O^\bullet$	1.298	1.232	2.448	1.289	1.240	2.450
$CH_3CH_2OCH_2O^\bullet$	1.297	1.238	2.437	1.286	1.248	2.438
$CH_3C(=O)OCH_2O^\bullet$	1.297	1.230	2.410	1.290	1.235	2.409

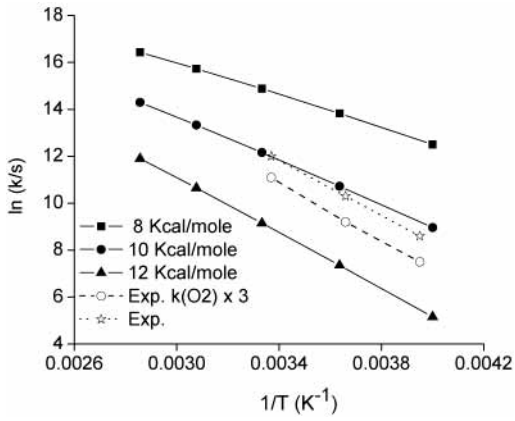

Figure 10. Calculated and experimental rate constants for the α-ester rearrangement in 1 atm of air. Calculated values are given assuming activation barriers of 8, 10, and 12 kcal/mol (at 0 K, including zero-point energy), which roughly spans the range of computed activation barriers. The experimental data are derived from the relative rate of the decomposition and O_2 reactions,[37,39] with the rate constant for the O_2 reaction assumed equal to that of the ethoxy radical at a given temperature[12] or three times that value.[2]

TABLE 9: Length of the Bonds Involved in the Transition State for Isomerization of Alkoxy Radicals at UMP2/6-31G(d), in Order of Increasing G2(UMP2,SVP) Barrier Height

reactant	$r(C_2-H_1)$	$r(O_6-H_1)$	$r(O_6-C_2)$
$CH_3OCH_2CH_2O^\bullet$	1.237	1.308	2.426
$CH_3OC(=O)CH_2O^\bullet$	1.233	1.262	2.393
$CH_3CH_2CH_2CH_2O^\bullet$	1.244	1.270	2.429
$CH_3CH_2C(=O)CH_2O^\bullet$	1.241	1.268	2.409
$CH_3C(=O)CH_2CH_2O^\bullet$	1.260	1.235	2.410
$CH_3CH_2OCH_2O^\bullet$	1.246	1.274	2.402
$CH_3C(=)OCH_2O^\bullet$	1.253	1.252	2.366

factor of 3 higher, as suggested by Aschmann and Atkinson, this activation barrier appears to be about 10 kcal/mol. The activation barriers to decomposition and isomerization imply rate constants of $\sim 5 \times 10^{-4}$ s^{-1} for both reactions: far too slow to compete with the O_2 reaction.

III. D. Effects of Tunneling on the Rate Constants. The above calculations of rate constants for isomerization and the α-ester rearrangement assume that quantum mechanical tunneling of the hydrogen atom is unimportant. The impact of tunneling can be estimated by modeling the reaction coordinate with asymmetric Eckart potential,[65,66] which commonly gives reasonable agreement with more exact computations of tunneling effects.[67] The ratio, $\Gamma(T)$ of the quantum mechanical versus classical rate constant for reactants at a thermal distribution of energy is given by

$$\Gamma(T) = \frac{\exp(V_1/k_BT)}{k_BT}\int_0^\infty \kappa(E)\exp(-E/k_BT)\,dE \qquad (8)$$

where κ(E) is the transmission probability. $\kappa(E)$ depends sensitively on the thickness of the barrier, as represented by the imaginary frequency, ν^*, of the vibration along the reaction coordinate. For the α-ester rearrangement, using activation barriers ranging from 8 to 12 kcal/mol, the B3LYP/6-31G(d,p) value of ν^* (493i cm^{-1}) results in $\Gamma(300\ K) = 1.3$, while the MP2/6-31G(d) value of ν^* (1229i cm^{-1}) results in $\Gamma(300\ K) = 5-6$. If an activation barrier of 10 kcal/mol at 0 K allows us to fit the experimental results, then after accounting for tunneling we see that the true activation barrier may be as high a 11 kcal/mol. If so, the G2(MP2,SVP) method has performed excellently in obtaining a barrier of 11.0−11.2 kcal/mol.

In a previous paper[68] we employed similar calculations for the 1,5 H-shift reaction of 1-butoxy radical (using the B3LYP/6-31G(d,p) imaginary frequency) to suggest a very large effect of tunneling: $\Gamma(298\ K) = 19$. Our present MP2/6-31G(d) results suggest $\Gamma(298\ K) = 210$. Note that these calculations are valid only in the high-pressure limit, and the 1,5 H-shift reaction is not in the high-pressure limit at 298 K and 1 atm (neither is the α-ester rearrangement). However, if these values of $\Gamma(298\ K)$ are approximately correct for the 1,5 H-shift, they imply a barrier height closer to 11.5−13.5 kcal/mol rather than the 10 kcal/mol calculated at B3LYP in this work or at G2(MP2,SVP) in ref 34. This means the apparent success of the B3LYP and G2(MP2,SVP) approaches,[25,30,34,35,51] cited in the Results and Discussion section, was somewhat deceiving. In the future we intend to look more carefully at tunneling effects on the rate constants for this and other H-atom transfer reactions, including the difference in the effect in the falloff region versus the high-pressure limit.

IV. Conclusions

Quantum chemical calculations lead to the prediction that reaction with O_2 will be the sole atmospheric fate of $CH_3CH_2OCH_2O^\bullet$ and $CH_3C(=O)CH_2CH_2O^\bullet$. For $CH_3OC(=O)CH_2O^\bullet$, reaction with O_2 is likely to be the dominant fate, although we are reluctant to conclude that isomerization is negligible. For $CH_3CH_2C(=O)CH_2O^\bullet$, we predict decomposition to be the sole fate. For $CH_3OCH_2CH_2O^\bullet$, decomposition and isomerization will both be much faster than the O_2 reaction, but isomerization appears to dominate over decomposition. A structure activity relationship (SAR) for the activation barrier to decomposition reaction was constructed, analogous to the one proposed by Atkinson. Although the values obtained for the two parameters in this SAR may be biased by the computational method, they suggest no role in the SAR for the ionization potential of the radical product of decomposition. These results, combined with estimates of other structural effects on the rate constants for the isomerization and decomposition reactions, will enable reasonable predictions of the importance of decomposition and isomerization reactions in a host of related alkoxy radicals. Tunneling appears to contribute enormously to the room-temperature rate constant for the 1,5 H-shift reaction, at least in 1-butoxy, a subject necessitating further research.

The concerted bond-breaking/H-atom transfer mechanism previously proposed for the α-ester rearrangement has been validated by these calculations, and the absence of a β-ester rearrangement has been rationalized. Tunneling may contribute significantly to the rate of the α-ester rearrangement.

Acknowledgment. The authors thank W. Deng for help with computers and for carrying out the UNIMOL calculations. We thank A. Sarko for his dedication to the maintenance of local computing facilities, J. P. Senosiain for giving us a copy of his spreadsheet for calculating tunneling corrections, and an anonymous reviewer for extensive comments on the manuscript. We further thank G. S. Tyndall and D. M. Golden for helpful discussions, and J. Andino for providing copies of papers prior to publication. This research was supported by the National Science Foundation under Grants ATM 9712381 and ATM 0087057. Further support was provided by the National Computational Science Alliance under Grants ATM980008N and ATM010003N and utilized the NCSA HP-Convex Exemplar SPP-2000 at the University of Illinois and the HP-N4000 cluster at the University of Kentucky.

Supporting Information Available: Tables of Cartesian coordinates for all species at the B3LYP/6-31G(d,p) level of

theory. This material is available free of charge via the Internet at http://pubs.acs.org.

References and Notes

(1) Singh, H.; Chen, Y.; Staudt, A.; Jacob, D.; Blake, D.; Heikes, B.; Snow, J. *Nature* **2001**, *410*, 1078.
(2) Aschmann, S. M.; Atkinson, R. *Int. J. Chem. Kinet.* **1999**, *31*, 501.
(3) Tuazon, E. C.; Aschmann, S. M.; Atkinson, R.; Carter, W. P. L. *J. Phys. Chem. A* **1998**, *102*, 2316.
(4) Stemmler, K.; Mengon, W.; Kerr, J. A. *Environ. Sci. Technol.* **1996**, *30*, 3385.
(5) Stemmler, K.; Mengon, W.; Kinnison, D. J.; Kerr, J. A. *Environ. Sci. Technol.* **1997**, *31*, 1496.
(6) Platz, J.; Sehested, J.; Nielsn, O. J.; Wallington, T. J. *J. Phys. Chem. A* **1999**, *103*, 2632.
(7) Maurer, T.; Hass, H.; Barnes, I.; Becker, K. H. *J. Phys. Chem. A* **1999**, *103*, 5032.
(8) Cheema, S. A.; Holbrook, K. A.; Oldershaw, G. A.; Starkey, D. P.; Walker, R. W. *Phys. Chem. Chem. Phys.* **1999**, *1*, 3243.
(9) Maurer, T.; Geiger, H.; Barnes, I.; Becker, K. H.; Thüner, L. P. *J. Phys. Chem. A* **2000**, *104*, 11087.
(10) Sempeles, J.; Andino, J. M. *Int. J. Chem. Kinet.* **2000**, *32*, 703.
(11) Atkinson, R. *J. Phys. Chem. Ref. Data Monograph 2*, **1994**.
(12) Atkinson, R. *Int. J. Chem. Kinet.* **1997**, *29*, 99.
(13) Jenkin, M. E.; Hayman, F. D. *Atmos. Environ.* **1999**, *33*, 1275.
(14) Grosjean, D.; Seinfeld, J. H. *Atmos. Environ.* **1989**, *23*, 1733.
(15) Sanders, N.; Butler, J. E.; Pasternack, L. R.; McDonald, J. R. *Chem Phys.* **1980**, *48*, 203.
(16) Lorenz, K.; Rhäsa, D.; Zellner, R.; Fritz, B. *Ber. Bunsen-Ges. Phys. Chem.* **1985**, *89*, 341.
(17) Balla, R. J.; Nelson, H. H.; McDonald, J. R. *Chem. Phys.* **1985**, *99*, 323.
(18) Hartmann, D.; Karthäuser, J.; Sawerysyn, J. P.; Zellner, R. *Ber. Bunsen-Ges. Phys. Chem.* **1990**, *94*, 639.
(19) Mund, Ch.; Fockenberg, Ch.; Zellner, R. *Ber. Bunsen-Ges. Phys. Chem.* **1998**, *102*, 709.
(20) Fittschen, C.; Frenzel, A.; Imrik, K.; Devolder, P. *Int. J. Chem. Kinet.* **1999**, *31*, 860.
(21) Deng, W.; Wang, C.-J.; Katz, D. R., Gawinski, G. A.; Davis, A. J.; Dibble, T. S. *Chem. Phys. Lett.* **2000**, *330*, 541.
(22) Deng, W.; Davis, A. J.; Zhang, L.; Katz, D. R., Dibble, T. S. *J. Phys. Chem. A* **2001**, *105*, 8985.
(23) Hein, H.; Hoffmann, A.; Zellner, R. *Phys. Chem. Chem. Phys.* **1999**, *1*, 3743.
(24) Baldwin, A. C.; Barker, J. R.; Golden, D. M.; Hendry, D. G. *J. Phys. Chem.* **1977**, *81*, 2483.
(25) Lendvay, G.; Viskolcz, B. *J. Phys. Chem. A* **1998**, *102*, 10777.
(26) Devolder, P.; Fittschen, Ch.; Frenzel, A.; Hippler, H.; Poskrebyshev, G.; Striebel, F.; Viskolcz, B. *Phys. Chem. Chem. Phys.* **1999**, *1*, 675.
(27) Caralp, F.; Devolder, P.; Fittschen, Ch.; Gomez, N.; Hippler, H.; Méreau, R.; Rayez, M. T.; Striebel, F.; Viskolcz, B. *Phys. Chem. Chem. Phys.* **1999**, *1*, 2935.
(28) Blitz, M.; Pilling, M. J.; Robertson, S. H.; Seakins, P. W. *Phys. Chem. Chem. Phys.* **1999**, *1*, 73.
(29) Fittschen, Ch.; Hippler, H.; Viskolcz, B. *Phys. Chem. Chem. Phys.* **2000**, *2*, 1677.
(30) Vereecken, L.; Peeters, J. *J. Phys. Chem A* **1999**, *103*, 1768.
(31) Méreau, R.; Rayez, M. T.; Caralp, F.; Rayez, J. C. *Phys. Chem. Chem. Phys.* **2000**, *2*, 1919.
(32) Vereecken, L.; Peeters, J.; Orlando, J. J.; Tyndall, G. S.; Ferronato, C. *J. Phys. Chem. A* **1999**, *103*, 4693.
(33) Somnitz, H.; Zellner, R. *Phys. Chem. Chem. Phys.* **1999**, *2*, 1899.
(34) Somnitz, H.; Zellner, R. *Phys. Chem. Chem. Phys.* **1999**, *2*, 1907.
(35) Somnitz, H.; Zellner, R. *Phys. Chem. Chem. Phys.* **2000**, *2*, 4319.
(36) Curtiss, L. A.; Redfern, P. C.; Smith, B. J.; Radom, L. *J. Chem. Phys.* **1996**, *104*, 5148.
(37) Christensen, L. K.; Ball, J. C.; Wallington, T. J. *J. Phys. Chem. A* **2000**, *104*, 345.
(38) Tuazon, E. C.; Aschmann, S. M.; Atkinson, R. *Environ. Sci. Technol.* **1999**, *33*, 2885.
(39) Tyndall, G. S.; Pimentel, A. S.; Orlando, J. J. Manuscript in preparation.
(40) *Spartan 4.0*; Wave function Inc., 18401 Von Karman Avenue, Suite 370, Irvine, CA 92612.
(41) Frisch, M. J.; Trucks, G. W.; Schlegel, H. B.; Gill, P. M. W.; Johnson, B. G.; Robb, M. A.; Cheeseman, J. R.; Keith, T.; Petersson, G. A.; Montgomery, J. A.; Raghavachari, K.; Al-Laham, M. A.; Zakrzewski, V. G.; Ortiz, J. V.; Foresman, J. B.; Cioslowski, J.; Stefanov, B. B.; Nanayakkara, A.; Challacombe, M.; Peng, C. Y.; Ayala, P. Y.; Chen, W.; Wong, M. W.; Andres, J. L.; Replogle, E. S.; Gomperts, R.; Martin, R. L.; Fox, D. J.; Binkley, J. S.; Defrees, D. J.; Baker, J.; Stewart, J. P.; Head-Gordon, M.; Gonzalez, C.; Pople, J. A. *Gaussian 94*, revision D.3; Gaussian, Inc.: Pittsburgh, PA, 1995.
(42) Frisch, M. J.; Trucks, G. W.; Schlegel, H. B.; Scuseria, G. E.; Robb, M. A.; Cheeseman, J. R.; Zakrzewski, V. G.; Montgomery, J. A., Jr.; Stratmann, R. E.; Burant, J. C.; Dapprich, S.; Millam, J. M.; Daniels, A. D.; Kudin, K. N.; Strain, M. C.; Farkas, O.; Tomasi, J.; Barone, V.; Cossi, M.; Cammi, R.; Mennucci, B.; Pomelli, C.; Adamo, C.; Clifford, S.; Ochterski, J.; Petersson, G. A.; Ayala, P. Y.; Cui, Q.; Morokuma, K.; Malick, D. K.; Rabuck, A. D.; Raghavachari, K.; Foresman, J. B.; Cioslowski, J.; Ortiz, J. V.; Stefanov, B. B.; Liu, G.; Liashenko, A.; Piskorz, P.; Komaromi, I.; Gomperts, R.; Martin, R. L.; Fox, D. J.; Keith, T.; Al-Laham, M. A.; Peng, C. Y.; Nanayakkara, A.; Gonzalez, C.; Challacombe, M.; Gill, P. M. W.; Johnson, B.; Chen, W.; Wong, M. W.; Andres, J. L.; Gonzalez, C.; Head-Gordon, M.; Replogle, E. S.; Pople, J. A. Gaussian 98, revision A.6; Gaussian, Inc.: Pittsburgh, PA, 1998.
(43) Lee, C.; Yang, W.; Parr, R. G. *Phys. Rev. B* **1988**, *37*, 785.
(44) Becke, A. D. *J. Chem. Phys.* **1993**, *98*, 5648.
(45) Curtiss, L. A.; Redfern, P. C.; Smith, B. J.; Radom, L. *J. Chem. Phys.* **1996**, *104*, 5148.
(46) Gilbert, R. G.; Smith, S. C.; Jordan, M. J. T. *UNIMOL Program Suite, (calculation of falloff curves for unimolecular and recombination reactions)*, 1993. Available from the authors, School of Chemistry, Sydney University, NSW 2006, Australia, or by e-mail to gilbert_r@summer.chem.su.oz.au.
(47) Gilbert, R. G.; Smith, S. C. *Theory of Unimolecular and Recombination Reactions*; Blackwell Scientific: Oxford, 1990; p 318.
(48) Orlando, J. J.; Tyndall, G. S.; Bilde, M.; Ferronato, C.; Wallington, T. J.; Vereecken, L.; Peeters, J. *J. Phys. Chem. A* **1998**, *102*, 8116.
(49) Dibble, T. S. *J. Phys. Chem. A* **1999**, *103*, 8559.
(50) Dibble, T. S. *Chem. Phys. Lett.* **1999**, *301*, 297.
(51) Jungkamp, T. P. W.; Smith, J. N.; Seinfeld, J. H. *J. Phys. Chem. A* **1997**, *101*, 4392.
(52) Lei, W.; Zhang, R. *J. Phys. Chem. A* **2001**, *105*, 3808.
(53) Reitz, J. E.; McGivern, W. S.; Church, M. C.; Wilson, M. D.; North, S. W. *Int. J. Chem. Kinet.* **2002**, *34*, 255.
(54) Hammond, G. S. *J. Am. Chem. Soc.* **1955**, *77*, 334.
(55) Fischer, H.; Radom, L. *Angew. Chem, Int. Ed.* **2001**, *40*, 1340.
(56) Donahue, N. M.; Clarke, J. S.; Anderson, J. G. *J. Phys. Chem. A* **1998**, *102*, 3923.
(57) Vereecken, L.; Peeters, J. *Chem. Phys. Lett.* **2001**, *333*, 162.
(58) Berkowitz, J.; Ellison, G. B.; Gutman, D. *J. Phys. Chem.* **1994**, *98*, 2744.
(59) Lias, S. G.; Bartmess, J. E.; Liebman, J. F.; Holmes, J. L.; Levin, R. D.; Mallard, W. G. *J. Phys. Chem. Ref. Data, Suppl. 1* **1988**, *17*, 1.
(60) Williams, J. M.; Hamill, W. H. *J. Chem. Phys.* **1968**, *49*, 4467.
(61) Kwok, E. S. C.; Atkinson R. *Atmos. Environ.* **1995**, *29*, 1685.
(62) Carter, W. P. L.; Lloyd, A. C.; Sprung, J. L.; Pitts, J. N., Jr. *Int. J. Chem. Kinet.* **1979**, *11*, 45.
(63) Cox, R. A.; Patrick, K. F.; Chant, S. A. *Environ. Sci. Technol.* **1981**, *15*, 587.
(64) Niki, H.; Maker, P. D.; Savage, C. M.; Breitenbach, L. P. *J. Phys. Chem.* **1981**, *85*, 2698.
(65) Eckhart, C. *Phys. Rev.* **1930**, *35*, 1303.
(66) Johnston, H. S. *Gas-Phase Reaction Rate Theory*; Ronald Press: New York, 1966.
(67) Senosiain, J. P.; Musgrave, C. B.; Golden, D. M. *J. Phys. Chem. A* **2001**, *105*, 1669.
(68) Dibble, T. S. *J. Phys. Chem. A* **2002**, *106*, 6643.